International Journal of Non–Linear Mechanics 163 (2024) 104749

Contents lists available at ScienceDirect

International Journal of Non-Linear Mechanics

journal homepage: www.elsevier.com/locate/nlm

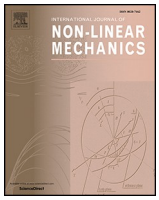

Nonlinear oscillation of microscale fiber-reinforced composite laminated beams under a thermal loading

Mehdi Alimoradzadeh [a], Francesco Tornabene [b,*], Rossana Dimitri [b]

[a] Department of Mechanical Engineering, Najafabad Branch, Islamic Azad University, Najafabad, Iran
[b] Department of Innovation Engineering, University of Salento, Lecce, Italy

ARTICLE INFO

Keywords:
Euler-Bernoulli beam theory
Fiber-reinforced composites
Modified couple stress theory
Nonlinear oscillation
Period-doubling bifurcation
Von kármán theory
Temperature dependent materials

ABSTRACT

The work analyzes the nonlinear dynamic response of fiber-reinforced composite laminated microbeams in thermal environment, accounting for the dependence of the material properties on temperature. The governing equations of the nonlinear partial differential equations are based on the Euler-Bernoulli beam theory, and the modified couple stress theory involving the von Kármán geometrical nonlinearity. The governing nonlinear equations are reduced to a single equation by neglecting the axial inertia, which is discretized in the form of nonlinear ordinary differential equation, according to the Galerkin method, and it is solved analytically using the multiple time scales (MTS) method. A systematic investigation checks for the effect of the material length scale parameter, temperature increase, and damping parameter of the microscale beam on its time history and phase plane trajectory. Different stacking sequences are also considered within the parametric investigation. Based on results, it is noticed that the system is in a damped period-doubling bifurcation for four cycle oscillation states. It is also noticed that the stacking sequence affects significantly the nonlinear dynamic behavior of the system. It is found that the microscale composite laminated beam with *[0/0/0]* lay-ups has the highest dynamical deflection and the highest nonlinear frequency, followed by *[0/90/0]*, [*30/-30/30]* (angle ply), *[90/0/90], [45/-45/45]* (angle ply) and *[60/-60/60]* (angle ply). However, the microscale composite laminated beam with *[90/90/90]* lay-ups has the lowest dynamical deflection and the lowest nonlinear frequency.

1. Introduction

The improved requirements of mechanical strength, low-density and sustainability of structures, have recently increased the use of composite sandwich structures, due to their outstanding engineering performances, i.e., high strength-to-weight ratio, corrosion resistance, thermal and acoustic insulation. In such a context, many structural examples of straight or curved beams, plates and shells can be found in many engineering applications, with optimized geometries and mechanical performances both in a static [1–4] and dynamic [5–11] sense.

From a dynamic perspective, a rapid increase of advanced theoretical and computational strategies has been observed in literature, even considering different environmental conditions. Among some recent works on the topic, a Runge-Kutta method was proposed by Duc and Cong [12] to study the vibrational response of composite plates in thermomechanical coupled loading conditions. A Galerkin decomposition technique was also proposed in Ref. [13] together with a multiple time scale method (MTS), to discretize and to solve the nonlinear partial differential equation governing the problem. Chai et al. [14] assessed the nonlinear vibration, bifurcation and chaos, of lattice sandwich structures with thermal effects in a supersonic air flow, while implementing a first-order shear deformation theory and von Kármán large deflection theory as structural models, together with a Runge-Kutta solution method, to determine time histories, phase maps, Poincaré plots and fast Fourier transform frequency spectra. A higher-order deformation beam theory was combined to a Rayleigh-Ritz method, by Ameri et al. [15] to investigate the effect of the honeycomb core on the free vibration of fiber metal laminate beams compared to more conventional composites. More recently, a third-order shear deformation theory was proposed by Amabili et al. [16] to model the nonlinear vibrations of cantilever beams made of self-healing materials, accounting for rotary inertia, in-plane and rotational nonlinearities in addition to traditional von Kármán nonlinear terms.

In the further works [17–22], a finite strain-based theory was applied to study the superharmonic and subharmonic resonance of composite beams in thermal conditions, under a moving mass loading. A

* Corresponding author.
E-mail address: francesco.tornabene@unisalento.it (F. Tornabene).

https://doi.org/10.1016/j.ijnonlinmec.2024.104749
Received 26 February 2024; Received in revised form 25 April 2024; Accepted 29 April 2024
Available online 1 May 2024

homogenization procedure based on a Mori–Tanaka scheme, was also combined to a first-order shear deformation theory in Ref. [23], for an accurate prediction of thermal frequency and buckling behavior of FGM beams, accounting for the micro-mechanical interaction of particles within mixtures. Among the size-dependent nonlinear dynamics of beam-like structures, some affine works from literature can be found in Refs. [24–28], based on nonlocal theories, such as the modified coupled stress theory, accounting for the effect of the material length scale parameter and power index on the overall response. Similarly, Civalek et al. [29] focused on the dynamic response of carbon and silica nanotubes embedded on an elastic matrix by means of the Eringen's nonlocal elasticity theory. Unlike macromechanical approaches, where composite materials are homogenized, micromechanical approaches distinguish matrix and fibers, and consider the effect of the matrix viscoelasticity on the homogenized properties of composites. In such a context, different micromechanical models rely on rules-of-mixtures [30], but also on different Halpin-Tsai [31], Mori–Tanaka [31], and Christensen [32] assumptions. At the same time, many recent works from literatures have focused their attention on the flutter instability of composite beams [33,34] and plates [35,36], using a Galerkin approach or a differential quadrature approach, including geometrical nonlinearities within the theoretical formulation, as recently proposed in Ref. [37], for the nonlinear axial-lateral vibration study of functionally graded-fiber reinforced composite laminated cantilever beams subjected to aero-thermal loads.

Accordingly to this last reference, the present work aims at studying the nonlinear oscillations of fiber-reinforced composite microbeams in a nonlocal sense, by employing a nonclassical modified couple stress theory together with the von Kármán geometrical nonlinearities. The nonlinear governing equations of the problem are solved in discrete form, according to the Galerkin method and MTS method. A systematic investigation focuses on the sensitivity of the time history and phase plane trajectory response of microbeams, on the material length scale parameter, temperature increase and damping parameters. The work is organized as follows: after this literature overview, we provide the theoretical framework of the problem in Section 2, whose numerical basics are detailed in Section 3. The numerical investigation is, thus, discussed in Section 4, with concluding remarks in Section 5.

2. Governing equations

Let consider a straight microscale fiber-reinforced composite laminated (FRCL) beam with length L, width b and thickness h, in x, y and z direction, respectively, as shown in Figs. (1) and (2). In the current study, we adopt a Euler-Bernoulli beam theory, in which the shear deformation is neglected together with the rotational and axial inertia of the beam. The FRCL beam is made by three layers with the same material with different lay-ups, which are perfectly bonded. The model considers a Von-Karman type geometric nonlinearity, where the FRCL microbeam is subjected to a uniform temperature rise, ΔT, and it is immersed within a viscous medium (Air damping). Moreover, the thermal expansion coefficients and elastic constants are assumed to depend on temperature.

According to the Euler-Bernoulli beam theory, the cross-sections of the beam remain orthogonal to the mid-plane after the deformation process, where the displacement field for an arbitrary point of the beam along the $x, y,$ and z directions, is defined as [38]

Fig. 1. Simply supported laminated microbeam under a uniform temperature rise ΔT.

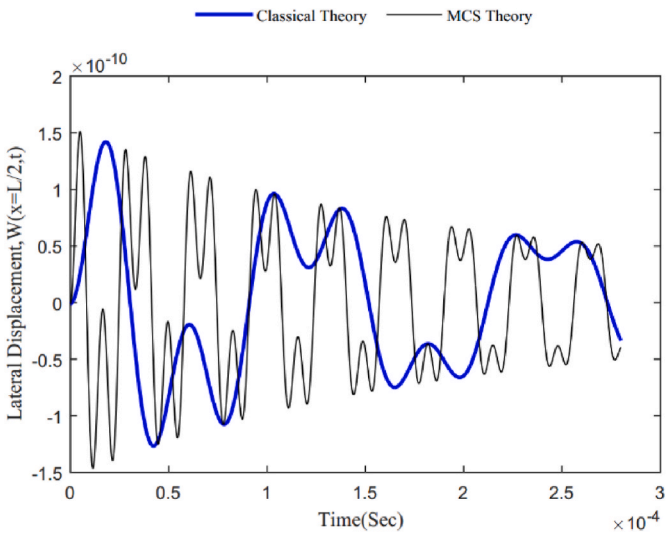

Fig. 2. Effect of length scale parameter on the time history of the microscale composite laminated beam.

$$u_x(x,z,t) = u(x,t) - z\frac{\partial w(x,t)}{\partial x} \tag{1}$$

$$u_y(x,z,t) = 0 \tag{2}$$

$$u_z(x,z,t) = w(x,t) \tag{3}$$

where $\frac{\partial w(x,t)}{\partial x}$ is the rotation angle of the cross section about the y axis and the arbitrary time t. The Von Kármán strain tensor is here adopted to consider the geometric nonlinearity.

Based on the Von Kármán strain tensor, the total nonlinear strain-displacement relationship can be defined as follows [39]

$$\varepsilon_{ij} = \frac{1}{2}\left[\frac{\partial u_i}{\partial j} + \frac{\partial u_j}{\partial i} + \frac{\partial u_z}{\partial i} \bullet \frac{\partial u_z}{\partial j}\right], (i,j,k)\ \epsilon\ [x,y,z] \tag{4}$$

Based on Eqs. (1)–(4), we get the following nonzero strain component

$$\varepsilon_{xx} = \frac{\partial u}{\partial x} - z\frac{\partial^2 w}{\partial x^2} + \frac{1}{2}\left(\frac{\partial w}{\partial x}\right)^2 \tag{5}$$

Based on the modified couple stress theory, the variation of the strain energy, δU_s, can be defined as [40]

$$\delta U_s = \int_0^L \int_A \left(\sigma_{ij}\delta\varepsilon_{ij} + m_{ij}\delta\chi_{ij}\right) dA dx, (\ i,j = x,y,z) \tag{6}$$

where δ, σ and A refer to the variational symbol, stress tensor and cross section area, respectively. Also, m and χ, are the deviatoric part of the symmetric couple stress tensor and the symmetric curvature tensor, respectively, defined as [40]

$$m_{ij} = \frac{1}{2}G_{12}l^2\chi_{ij} \tag{7}$$

$$\chi_{ij} = \frac{1}{2}\left(\frac{\partial \theta_i}{\partial j} + \frac{\partial \theta_j}{\partial i}\right) \tag{8}$$

where G_{12} is a composite material constant, l is a material length scale parameter, introduced to characterize the couple stress effect, and θ denotes the rotation vector and can be written as [40]

$$\theta = \left\{\frac{1}{2}\left(\frac{\partial u_z}{\partial y} - \frac{\partial u_y}{\partial z}\right), \frac{1}{2}\left(\frac{\partial u_x}{\partial z} - \frac{\partial u_z}{\partial x}\right), \frac{1}{2}\left(\frac{\partial u_y}{\partial x} - \frac{\partial u_x}{\partial y}\right)\right\} \tag{9}$$

Substituting Eqs. (1)–(3) into Eq. (9) leads to

$$\theta_x = \theta_z = 0\ \theta_y = -\frac{\partial w}{\partial x} \tag{10}$$

Substituting Eq. (10) into Eq. (8), leads to the nonzero components of the symmetric curvature tensor as below

$$\chi_{xy} = \chi_{yx} = -\frac{1}{2}\frac{\partial^2 w}{\partial x^2} \tag{11}$$

Since the non-zero parts of the strain tensor and the curvature tensor are ε_{xx} and $\chi_{xy} = \chi_{yx}$ respectively, Eq. (6) takes the following form

$$\delta U_s = \int_0^L \int_A \left(\sigma_{xx}\delta\varepsilon_{xx} + 2m_{xy}\delta\chi_{xy}\right) dA dx \tag{12}$$

In presence of a thermal load, the axial stress-strain relationship of the k-th layer can be expressed as [41]

$$\sigma_{xx}^{(k)} = \overline{Q}_{11}^{(k)}\left(\varepsilon_{xx} - \alpha_x^{(k)}\Delta T\right) + \overline{Q}_{12}^{(k)}\left(\varepsilon_{yy} - \alpha_y^{(k)}\Delta T\right) + \overline{Q}_{16}^{(k)}\left(\varepsilon_{xy} - \alpha_{xy}^{(k)}\Delta T\right) \tag{13}$$

$\overline{Q}_{11}^{(k)}$, $\overline{Q}_{12}^{(k)}$ and $\overline{Q}_{16}^{(k)}$ being the transformed reduced stiffnesses, defined as [38]

$$\begin{aligned}\overline{Q}_{11}^{(k)} &= Q_{11}^k c^4 + Q_{22}^k s^4 + 2\left(Q_{12}^k + 2Q_{66}^k\right)s^2c^2\ \overline{Q}_{12}^{(k)} = \left(Q_{11}^k + Q_{22}^k\right.\\ &\left. - 4Q_{66}^k\right)s^2c^2 + Q_{12}^k\left(s^4 + c^4\right)\ \overline{Q}_{16}^{(k)} = \left(Q_{11}^k - Q_{12}^k - 2Q_{66}^k\right)sc^3 + \left(Q_{12}^k\right.\\ &\left. - Q_{22}^k + 2Q_{66}^k\right)cs^3\end{aligned} \tag{14}$$

whereas Q_{11}^k, Q_{12}^k, Q_{22}^k and Q_{66}^k are the reduced stiffnesses properties expressed as [41]

$$Q_{11}^k = \frac{E_1^k}{\left(1 - \vartheta_{12}^k\vartheta_{21}^k\right)}\ Q_{12}^k = \frac{\vartheta_{12}^k E_2^k}{\left(1 - \vartheta_{12}^k\vartheta_{21}^k\right)}\ Q_{22}^k = \frac{E_2^k}{\left(1 - \vartheta_{12}^k\vartheta_{21}^k\right)}\ Q_{66}^k = G_{12}^k\ \vartheta_{21}^k = \frac{\vartheta_{12}^k E_{22}^k}{E_{11}^k} \tag{15}$$

In the previous equations, E_1^k and E_2^k represent the elastic modulus along and orthogonally the fiber direction, respectively, G_{12}^k is the shear moduli, whereas ϑ_{12}^k and ϑ_{21}^k are the Poisson's ratios at the k-th layer. Also $\alpha_x^{(k)}$, $\alpha_y^{(k)}$ and $\alpha_{xy}^{(k)}$ refer to the of the thermal deformation coefficients in the global coordinate system, defined as [41]

$$\alpha_x^{(k)} = \alpha_1^k c^2 + \alpha_2^k s^2\ \alpha_y^{(k)} = \alpha_1^k s^2 + \alpha_2^k c^2\ \alpha_{xy}^{(k)} = 2\left(\alpha_1^k - \alpha_2^k\right)sc \tag{16}$$

with α_1^k and α_2^k, the thermal expansion coefficients along the longitudinal and transverse direction of fibers, respectively. Also, $c = \cos\theta^k, s = \sin\theta^k$ and θ^k refer to the angle of the fibers with respect to the x-axis.

Except for the Poisson's ratio which can be reasonably assumed constant, the material properties for each layer are considered as linear functions of temperature. For Graphite/Epoxy, the thermo-mechanical properties can be expressed as [42,43].

$$\begin{aligned}E_1^k &= 155\left(1 - 3.53\times10^{-4}\Delta T\right)GPa\ E_2^k = 8.07\left(1\right.\\ &\left. - 4.27\times10^{-4}\Delta T\right)GPa\ G_{12}^k = G_{13}^k = 4.55\left(1\right.\\ &\left. - 6.06\times10^{-4}\Delta T\right)GPa\ G_{23}^k = 3.25\left(1 - 6.06\times10^{-4}\Delta T\right)GPa\ \alpha_1^k =\\ &- 0.07\times10^{-6}\left(1\right.\\ &\left. - 1.25\times10^{-3}\Delta T\right)\ {}^1/_{C^\circ}\ \alpha_2^k = 30.1\times10^{-6}\left(1 + 0.41\times10^{-4}\Delta T\right)\ {}^1/_{C^\circ}\ \vartheta_{12} = 0.22\end{aligned} \tag{17}$$

where ΔT is the uniform temperature rise throughout the thickness of the beam. By substitution of Eqs. ((5), (7), (11) and (13) into Eq. (12) and recalling that $\varepsilon_{yy} = \varepsilon_{xy} = 0$, leads to

$$\begin{aligned}\delta U_s &= b\int_0^L \left[\sum_{k=1}^{n=3}\int_{z_{k-1}}^{z_k}\left(\sigma_{xx}\delta\varepsilon_{xx} + 2m_{xy}\delta\chi_{xy}\right)dz\right]dx = b\int_0^L \sum_{k=1}^{3}\int_{z_{k-1}}^{z_k}\left\{\left[\overline{Q}_{11}^{(k)}\left(\varepsilon_{xx}\right.\right.\right.\\ &\left. - \alpha_x^{(k)}\Delta T\right) - \overline{Q}_{12}^{(k)}\alpha_y^{(k)}\Delta T - \overline{Q}_{16}^{(k)}\alpha_{xy}^{(k)}\Delta T\Big]\delta\left(\frac{\partial u}{\partial x}\right) + \left[\overline{Q}_{11}^{(k)}\left(\varepsilon_{xx} - \alpha_x^{(k)}\Delta T\right)\right.\\ &\left. - \left(\overline{Q}_{12}^{(k)}\alpha_y^{(k)} + \overline{Q}_{16}^{(k)}\alpha_{xy}^{(k)}\right)\Delta T\right]\frac{\partial w}{\partial x}\delta\left(\frac{\partial w}{\partial x}\right) - \Big[\Big(\overline{Q}_{11}^{(k)}\left(\varepsilon_{xx} - \alpha_x^{(k)}\Delta T\right)\\ &\left. - \left(\overline{Q}_{12}^{(k)}\alpha_y^{(k)} + \overline{Q}_{16}^{(k)}\alpha_{xy}^{(k)}\right)\Delta T\Big)z - \frac{1}{4}G_{12}l^2\frac{\partial^2 w}{\partial x^2}\Big]\delta\left(\frac{\partial^2 w}{\partial x^2}\right)\right\}dz dx\end{aligned} \tag{18}$$

$$\begin{aligned}&= \int_0^L \left\{\left[A_{11}\left(\frac{\partial u}{\partial x} + \frac{1}{2}\left(\frac{\partial w}{\partial x}\right)^2\right) - B_{11}\frac{\partial^2 w}{\partial x^2} + \overline{N}_T\right]\delta\left(\frac{\partial u}{\partial x}\right)\right.\\ &\quad + \left[A_{11}\left(\frac{\partial u}{\partial x} + \frac{1}{2}\left(\frac{\partial w}{\partial x}\right)^2\right)\right.\\ &\quad \left. - B_{11}\frac{\partial^2 w}{\partial x^2} + \overline{N}_T\right]\frac{\partial w}{\partial x}\delta\left(\frac{\partial w}{\partial x}\right)\\ &\quad + \left[\left(D_{11} - \gamma\right)\frac{\partial^2 w}{\partial x^2} - B_{11}\left(\frac{\partial u}{\partial x} + \frac{1}{2}\left(\frac{\partial w}{\partial x}\right)^2\right)\right.\\ &\quad \left.\left. - \overline{M}_T\right]\delta\left(\frac{\partial^2 w}{\partial x^2}\right)\right\}dx\end{aligned} \tag{19}$$

$$\begin{aligned}&= -\int_0^L \left\{\left(\frac{\partial}{\partial x}\left[A_{11}\left(\frac{\partial u}{\partial x} + \frac{1}{2}\left(\frac{\partial w}{\partial x}\right)^2\right)\right.\right.\right.\\ &\quad \left. - B_{11}\frac{\partial^2 w}{\partial x^2} + \overline{N}_T\right]\Big)\delta u + \left(\frac{\partial}{\partial x}\left[A_{11}\left(\frac{\partial u}{\partial x} + \frac{1}{2}\left(\frac{\partial w}{\partial x}\right)^2\right)\right.\right.\\ &\quad \left. - B_{11}\frac{\partial^2 w}{\partial x^2} + \overline{N}_T\right]\frac{\partial w}{\partial x} + \frac{\partial^2 w}{\partial x^2}\left[A_{11}\left(\frac{\partial u}{\partial x} + \frac{1}{2}\left(\frac{\partial w}{\partial x}\right)^2\right) - B_{11}\frac{\partial^2 w}{\partial x^2} + \overline{N}_T\right]\\ &\quad - \frac{\partial^2}{\partial x^2}\left[\left(D_{11} - \gamma\right)\frac{\partial^2 w}{\partial x^2} - B_{11}\left(\frac{\partial u}{\partial x} + \frac{1}{2}\left(\frac{\partial w}{\partial x}\right)^2\right)\right.\\ &\quad \left.\left.\left. - \overline{M}_T\right]\right)\delta w\right\}dx + \left[A_{11}\left(\frac{\partial u}{\partial x} + \frac{1}{2}\left(\frac{\partial w}{\partial x}\right)^2\right) - B_{11}\frac{\partial^2 w}{\partial x^2} + \overline{N}_T\right]\delta u\Big|_0^L\\ &\quad + \left[\left(D_{11} - \gamma\right)\frac{\partial^2 w}{\partial x^2} - B_{11}\left(\frac{\partial u}{\partial x} + \frac{1}{2}\left(\frac{\partial w}{\partial x}\right)^2\right) - \overline{M}_T\right]\delta\left(\frac{\partial w}{\partial x}\right)\Big|_0^L\\ &\quad + \left(\frac{\partial w}{\partial x}\left[A_{11}\left(\frac{\partial u}{\partial x} + \frac{1}{2}\left(\frac{\partial w}{\partial x}\right)^2\right) - B_{11}\frac{\partial^2 w}{\partial x^2} + \overline{N}_T\right]\right.\\ &\quad \left. - \frac{\partial}{\partial x}\left[\left(D_{11} - \gamma\right)\frac{\partial^2 w}{\partial x^2} - B_{11}\left(\frac{\partial u}{\partial x} + \frac{1}{2}\left(\frac{\partial w}{\partial x}\right)^2\right) - \overline{M}_T\right]\right)\delta w\Big|_0^L\end{aligned} \tag{20}$$

where

$$\begin{aligned}\overline{N}_T &= -b\Delta T\left(\sum_{k=1}^{3}\int_{z_{k-1}}^{z_k}\overline{Q}_{11}^{(k)}\alpha_x^{(k)}dz + \sum_{k=1}^{3}\int_{z_{k-1}}^{z_k}\overline{Q}_{12}^{(k)}\alpha_y^{(k)}dz + \sum_{k=1}^{3}\right.\\ &\quad \left.\times\int_{z_{k-1}}^{z_k}\overline{Q}_{16}^{(k)}\alpha_{xy}^{(k)}dz\right)\ \overline{M}_T = -b\Delta T\left(\sum_{k=1}^{3}\int_{z_{k-1}}^{z_k}\overline{Q}_{11}^{(k)}\alpha_x^{(k)}z dz + \sum_{k=1}^{3}\right.\\ &\quad \left.\times\int_{z_{k-1}}^{z_k}\overline{Q}_{12}^{(k)}\alpha_y^{(k)}z dz + \sum_{k=1}^{3}\int_{z_{k-1}}^{z_k}\overline{Q}_{16}^{(k)}\alpha_{xy}^{(k)}z dz\right)\gamma = -b\sum_{k=1}^{3}\\ &\quad \times\int_{z_{k-1}}^{z_k}\frac{1}{4}G_{12}l^2 dz\ A_{11}, B_{11}, D_{11} = b\sum_{k=1}^{3}\int_{z_{k-1}}^{z_k}\overline{Q}_{11}^{(k)}\left(1, z, z^2\right)dz\end{aligned} \tag{21}$$

In the equations above, A_{11}, B_{11} and D_{11} refer to the axial, axial-bending, and bending stiffness of the beam, respectively.

The first variation of the kinetic energy of the composite laminate beam is defined as [44].

$$\delta K = \int_0^L \int_{-\frac{b}{2}}^{\frac{b}{2}} \left[\sum_{k=1}^{n} \int_{Z_{k-1}}^{Z_k} \rho^{(k)} \left(\frac{\partial u}{\partial t}\right)^T \delta\left(\frac{\partial u}{\partial t}\right) dz \right] dy dx \tag{22}$$

$\rho^{(k)}$ being the density for the k-th layer of the beam material. Using the displacement field shown in Eqs. (1)–(3) and Eq. (22), the first variation of the kinetic energy on the domain [0,T] is obtained as

$$\begin{aligned}\int_0^T \delta K dt = &\int_0^T \left(\left[I_1 \frac{\partial^2 u}{\partial t^2} - I_2 \frac{\partial^3 w}{\partial x \partial t^2} \right] \delta w \Big| \begin{matrix} L \\ 0 \end{matrix} \right) dt + \int_0^L \left\{ \left(\left[I_0 \frac{\partial u}{\partial t} - I_1 \frac{\partial^2 w}{\partial x \partial t} \right] \delta u \right.\right. \\ &- \left[I_1 \frac{\partial u}{\partial t} - I_2 \frac{\partial^2 w}{\partial x \partial t} \right] \delta\left(\frac{\partial w}{\partial x}\right) + \left[I_0 \frac{\partial w}{\partial t} \right] \delta w \Big) \Big| \begin{matrix} T \\ 0 \end{matrix} \Big\} dx - \int_0^T \int_0^L \left\{ \left[I_0 \frac{\partial^2 u}{\partial t^2} \right.\right. \\ &\left.\left. - I_1 \frac{\partial^3 w}{\partial x \partial t^2} \right] \delta u + \left[I_0 \frac{\partial w}{\partial t} \right] \delta w \Big) \Big| \begin{matrix} T \\ 0 \end{matrix} \Big\} dx - \int_0^T \int_0^L \left\{ \left[I_0 \frac{\partial^2 u}{\partial t^2} - I_1 \frac{\partial^3 w}{\partial x \partial t^2} \right] \delta u \right. \\ &\left. + \left[I_0 \frac{\partial^2 w}{\partial t^2} + \frac{\partial}{\partial x} \left(I_1 \frac{\partial^2 u}{\partial t^2} - I_2 \frac{\partial^3 w}{\partial x \partial t^2} \right) \right] \delta w \right\} dx\, dt \end{aligned} \tag{23}$$

where

$$b \sum_{k=1}^{n=3} \int_{z_{k-1}}^{z_k} \rho^{(k)} (1, z, z^2) dz = I_0, I_1, I_2$$

The first variation of virtual work associated to the external forces acting on the beam can be defined as [39]

$$\delta W^{Ext} = \int_0^L [F_u(x,t)\delta u + F_w(x,t)\delta w] dx + \left[\overline{N}\delta u + \overline{V}\delta w + \overline{M}\delta\left(\frac{\partial w}{\partial x}\right) \right] \Big| \begin{matrix} x = L \\ x = 0 \end{matrix} \tag{24}$$

where F_u and $F_w = F_d$ are the external force components distributed along the x and z direction, respectively. Also, $\overline{N}$, $\overline{V}$ and $\overline{M}$ are the axial force, transverse shear force, and bending moment, respectively, acting on the end sections of the beam. Moreover, F_d, is the damping force due to the viscous medium (Air damping) and it is defined as

$$F_d = c_d \frac{\partial w}{\partial t} \tag{25}$$

c_d being the coefficient of the viscous damping.

The governing equation of the system beam can be obtained from the Hamilton's principle as [41]

$$\delta \int_0^T [K - U_s + W^{Ext}] dt = 0 \tag{26}$$

δ is the variational symbol. Substituting Eqs. (20), (23a) and (24) into Eq. (26) leads to the following governing equations

$$\frac{\partial}{\partial x} \left[A_{11} \left(\frac{\partial u}{\partial x} + \frac{1}{2} \left(\frac{\partial w}{\partial x} \right)^2 \right) - B_{11} \frac{\partial^2 w}{\partial x^2} + \overline{N}_T \right] + F_u = I_0 \frac{\partial^2 u}{\partial t^2} - I_1 \frac{\partial^3 w}{\partial x \partial t^2} \tag{27}$$

$$\begin{aligned} &\frac{\partial}{\partial x} \left[A_{11} \left(\frac{\partial u}{\partial x} + \frac{1}{2} \left(\frac{\partial w}{\partial x} \right)^2 \right) \right. \\ &\left. - B_{11} \frac{\partial^2 w}{\partial x^2} + \overline{N}_T \right] \left(\frac{\partial w}{\partial x} \right) + \frac{\partial^2 w}{\partial x^2} \left[A_{11} \left(\frac{\partial u}{\partial x} + \frac{1}{2} \left(\frac{\partial w}{\partial x} \right)^2 \right) - B_{11} \frac{\partial^2 w}{\partial x^2} + \overline{N}_T \right] \\ &- \frac{\partial^2}{\partial x^2} \left[(D_{11} - \gamma) \frac{\partial^2 w}{\partial x^2} - B_{11} \left(\frac{\partial u}{\partial x} + \frac{1}{2} \left(\frac{\partial w}{\partial x} \right)^2 \right) - \overline{M}_T \right] + F_w = I_0 \frac{\partial^2 w}{\partial t^2} \\ &+ \frac{\partial}{\partial x} \left(I_1 \frac{\partial^2 u}{\partial t^2} - I_2 \frac{\partial^3 w}{\partial x \partial t^2} \right) \end{aligned} \tag{28}$$

At the same time, the related boundary conditions at $x = 0$ and $x = L$ are obtained as

$$\overline{N} = \left[A_{11} \left(\frac{\partial u}{\partial x} + \frac{1}{2} \left(\frac{\partial w}{\partial x} \right)^2 \right) - B_{11} \frac{\partial^2 w}{\partial x^2} + \overline{N}_T \right] \text{ or } \delta u = 0 \tag{29}$$

$$\begin{aligned} \overline{V} = &\frac{\partial w}{\partial x} \left[A_{11} \left(\frac{\partial u}{\partial x} + \frac{1}{2} \left(\frac{\partial w}{\partial x} \right)^2 \right) - B_{11} \frac{\partial^2 w}{\partial x^2} + \overline{N}_T \right] - \frac{\partial}{\partial x} \left[(D_{11} - \gamma) \frac{\partial^2 w}{\partial x^2} \right. \\ &\left. - B_{11} \left(\frac{\partial u}{\partial x} + \frac{1}{2} \left(\frac{\partial w}{\partial x} \right)^2 \right) - \overline{M}_T \right] - \left[I_1 \frac{\partial^2 u}{\partial t^2} - I_2 \frac{\partial^3 w}{\partial x \partial t^2} \right] \quad Or\ \delta w = 0 \end{aligned} \tag{30}$$

$$\overline{M} = \left[(D_{11} - \gamma) \frac{\partial^2 w}{\partial x^2} - B_{11} \left(\frac{\partial u}{\partial x} + \frac{1}{2} \left(\frac{\partial w}{\partial x} \right)^2 \right) - \overline{M}_T \right] \text{ or } \delta \left(\frac{\partial w}{\partial x} \right) = 0 \tag{31}$$

In order to obtain a solitary equation in terms of the lateral displacement, the contribution of the axial and the rotational inertia are neglected [37,45]. Moreover, as mentioned before the system is subjected to a uniform temperature rise. In other words, $F_u = 0$ and $F_w = F_d$. Therefore, Eqs. (27) and (28) take the following form

$$\frac{\partial}{\partial x} \left[A_{11} \left(\frac{\partial u}{\partial x} + \frac{1}{2} \left(\frac{\partial w}{\partial x} \right)^2 \right) - B_{11} \frac{\partial^2 w}{\partial x^2} + \overline{N}_T \right] = 0 \tag{32}$$

$$\begin{aligned} &\frac{\partial^2}{\partial x^2} \left[(D_{11} - \gamma) \frac{\partial^2 w}{\partial x^2} - B_{11} \left(\frac{\partial u}{\partial x} + \frac{1}{2} \left(\frac{\partial w}{\partial x} \right)^2 \right) - \overline{M}_T \right] \\ &- \frac{\partial^2 w}{\partial x^2} \left[A_{11} \left(\frac{\partial u}{\partial x} + \frac{1}{2} \left(\frac{\partial w}{\partial x} \right)^2 \right) - B_{11} \frac{\partial^2 w}{\partial x^2} + \overline{N}_T \right] - \frac{\partial}{\partial x} \left[A_{11} \left(\frac{\partial u}{\partial x} + \frac{1}{2} \left(\frac{\partial w}{\partial x} \right)^2 \right) \right. \\ &\left. - B_{11} \frac{\partial^2 w}{\partial x^2} + \overline{N}_T \right] \left(\frac{\partial w}{\partial x} \right) + I_0 \frac{\partial^2 w}{\partial t^2} + C_d \frac{\partial w}{\partial t} = 0 \end{aligned} \tag{33}$$

Eq. (32) can be redefined as

$$\frac{\partial^2 u}{\partial x^2} = \frac{\partial}{\partial x} \left[-\frac{1}{2} \left(\frac{\partial w}{\partial x} \right)^2 + \frac{B_{11}}{A_{11}} \frac{\partial^2 w}{\partial x^2} \right] \tag{34}$$

Integrating Eq. (34) with respect to the x-axis yields

$$\frac{\partial u}{\partial x} = -\frac{1}{2} \left(\frac{\partial w}{\partial x} \right)^2 + \frac{B_{11}}{A_{11}} \frac{\partial^2 w}{\partial x^2} - \frac{N_0(t)}{A_{11}} \tag{35}$$

which is integrated once again to yield

$$u(x,t) = \int_0^x -\frac{1}{2} \left(\frac{\partial w}{\partial x} \right)^2 dx + \frac{B_{11}}{A_{11}} \frac{\partial w}{\partial x} - \frac{N_0 x}{A_{11}} + N_1(t) \tag{36}$$

where N_0 and N_1 are two constants of integration, that are determined enforcing two boundary conditions. The microscale beam has immovable supports, such that

$$u(0,t) = u(L,t) = 0 \tag{37}$$

By substituting Eq. (37) into Eq. (36), we get the following expressions for N_0 and N_1.

$$N_0 = -\frac{A_{11}}{2L} \int_0^L \left(\frac{\partial w}{\partial x} \right)^2 dx + \frac{B_{11}}{L} \left[\frac{\partial w(L,t)}{\partial x} - \frac{\partial w(0,t)}{\partial x} \right] \tag{38}$$

$$N_1 = -\frac{B_{11}}{A_{11}} \frac{\partial w(0,t)}{\partial x} \tag{39}$$

Finally, by substituting Eqs. (32) and (35) into Eq. (33), we obtain the following nonlinear partial differential equation governing the motion of the fiber-reinforced composite laminated beams, namely

$$I_0 \frac{\partial^2 w}{\partial t^2} + C_d \frac{\partial w}{\partial t} + \left[D_{11} - \frac{{B_{11}}^2}{A_{11}} - \gamma \right] \frac{\partial^4 w}{\partial x^4} + (N_0 - \overline{N}_T) \frac{\partial^2 w}{\partial x^2} = 0 \tag{40}$$

To convert Eq. (40) into an ordinary differential equation, we apply the Galerkin method with one term approximation, as follows [46]

$$w(x,t)=\psi(x)q(t) \tag{41}$$

where $\psi(x)$ is the first and the most dominant modal function of linear vibration in lateral direction. Also, $q(t)$, is a time dependent modal coefficient that must be determined. For a simply-supported beam, the lateral mode shape function can be expressed as below [47]

$$\psi(x)=sin\left(\frac{\pi x}{L}\right) \tag{42}$$

Substituting Eq. (41) into Eq. (40) yields

$$I_0\psi\ddot{q}+C_d\psi\dot{q}+a_1q+a_2q^2+a_3q^3 \tag{43}$$

where the dot symbol refers to derivatives with respect to time. Also, the coefficients a_1, a_2, and a_3 are

$$a_1=\left[\psi_{,xxxx}\left(D_{11}-\frac{{B_{11}}^2}{A_{11}}-\gamma\right)-\psi_{,xx}\overline{N}_T\right]\ a_2=\frac{B_{11}}{L}\psi_{,xx}[\psi_x(L)-\psi_x(0)]\ a_3=\psi_{,xx}\left[-\frac{A_{11}}{2L}\int_0^L{\psi_x}^2dx\right] \tag{44}$$

The terms with x indices refer to derivatives with respect to x. Multiplying Eq. (43) with mode shape function $\psi(x)$ and integrating over the domain $(0, L)$, leads to the nonlinear ordinary differential equation governing the microscale composite beams as below

$$\ddot{q}+2\widehat{\mu}\dot{q}+\omega_0^2q+\widehat{\eta}_2q^2+\widehat{\eta}_3q^3=0 \tag{45}$$

where

$$\widehat{\mu}=\frac{1}{2}\left(\frac{\int_0^L C_d\psi^2dx}{\int_0^L I_0\psi^2(x)dx}\right) \tag{46}$$

$$\omega_0^2=\frac{\int_0^L a_1\psi(x)dx}{\int_0^L I_0\psi^2(x)dx} \tag{47}$$

$$\widehat{\eta}_2=\frac{\int_0^L a_2\psi(x)dx}{\int_0^L I_0\psi^2(x)dx} \tag{48}$$

$$\widehat{\eta}_3=\frac{\int_0^L a_3\psi(x)dx}{\int_0^L I_0\psi^2(x)dx} \tag{49}$$

Eq. (45) is the nonlinear ordinary differential equation governing the motion of the system and can be solved by using the MTS method [48]. First to achieve a uniformly valid approximate solution the following assumptions can be considered

$$\widehat{\mu}=\epsilon^2\mu\ \widehat{\eta}_2=\epsilon\eta_2\ \widehat{\eta}_3=\epsilon^2\eta_3 \tag{50}$$

$\epsilon\ll1$, is a dimensionless parameter and acts as a key parameter. Substituting Eq. (50) into Eq. (45) yields

$$\ddot{q}+2\epsilon^2\mu\dot{q}+\omega_0^2q+\epsilon\eta_2q^2+\epsilon^2\eta_3q^3=0 \tag{51}$$

Following the MTS method, the new independent time variables can be introduced as below [48]

$$T_n=\epsilon^nt,n=0,1,2,3,.. \tag{52}$$

Therefore, the derivatives with respect to time takes the following form according to the chain rule

$$\frac{d}{dt}=D_0+\epsilon D_1+\epsilon^2D_2+\epsilon^3D_3+\ldots\ \frac{d^2}{dt^2}=D_0^2+2\epsilon D_0D_1+\epsilon^2\left(D_1^2+2D_0D_2\right)+2\epsilon^3(D_1D_2)+\ldots \tag{53}$$

where

$$D_i=\frac{\partial}{\partial T_i},i=0,1,2,3,\ldots.$$

Based on the MTS method, the solution of Eq. (51) can be expressed as [47]

$$q(\epsilon,t)=q_0(T_0,T_1,T_2)+\epsilon q_1(T_0,T_1,T_2)+\epsilon^2q_2(T_0,T_1,T_2)+\ldots \tag{54}$$

By substitution of Eq. (54) into Eq. (51) together with Eq. (53), and by equating the coefficients of similar power of ϵ to zero yields

$$\left(D_0^2+\omega_0^2\right)q_0=0 \tag{55}$$

$$\left(D_0^2+\omega_0^2\right)q_1=-2D_0D_1q_0-\eta_2q_0^2 \tag{56}$$

$$\left(D_0^2+\omega_0^2\right)q_2=-2D_0D_1q_1-\left(D_1^2+2D_0D_2\right)q_0-2\mu D_0q_0-2\eta_2q_0q_1-\eta_3q_0^3 \tag{57}$$

The general solution of Eq. (55) can be expressed as

$$q_0=A(T_1,T_2)e^{i\omega_0T_0}+\overline{A}(T_1,T_2)e^{-i\omega_0T_0} \tag{58}$$

where $A(\mathrm{T}_1,\mathrm{T}_2)$ is an unknown complex function and will be determined by eliminating the secular terms from q_1 and q_2. Also $\overline{A}$ is the complex conjugate of A. Substituting Eq. (58) into Eq. (56) yields

$$\left(D_0^2+\omega_0^2\right)q_1=-2i\omega_0D_1A\ e^{i\omega_0T_0}-\eta_2\left[A^2e^{2i\omega_0T_0}+A\overline{A}\right]+cc \tag{59}$$

where cc stands for the complex conjugate of the previous terms. Thus, we eliminate the secular terms from q_1 equating the coefficients of $e^{\mp i\omega_0T_0}$ in Eq. (59) to zero as follows

$$2i\omega_0D_1A=0 \tag{60}$$

such that

$$A=A(T_2) \tag{61}$$

By considering Eq. (60), the particular solution of Eq. (59) can be defined as below

$$q_1=\frac{\eta_2}{3\omega_0^2}\left[A^2e^{2i\omega_0T_0}+\overline{A}^2e^{-2i\omega_0T_0}-6A\overline{A}\right] \tag{62}$$

By substituting Eq. (58), and (62) into Eq. (57), and enforcing $D_1A=0$, yields

$$\left(D_0^2+\omega_0^2\right)q_2=-A^3\left[\frac{2\eta_2^2}{3\omega_0^2}+\eta_3\right]e^{3i\omega_0T_0}+\left[-2i\omega_0(D_2A+\mu A)+A^2\overline{A}\left(\frac{10\eta_2^2}{3\omega_0^2}-3\eta_3\right)\right]e^{i\omega_0T_0}+cc \tag{63}$$

To eliminate the secular terms from q_2 equating the coefficients of $e^{\mp i\omega_0T_0}$ in Eq. (63) to zero as follows

$$-2i\omega_0(D_2A+\mu A)+A^2\overline{A}\left(\frac{10\eta_2^2}{3\omega_0^2}-3\eta_3\right)=0 \tag{64}$$

Let consider $A(T_2)$ in the polar form as follows [48]

$$A(T_2)=\frac{1}{2}a\ e^{i\beta} \tag{65}$$

a and β are real functions of T_2. Substituting Eq. (65) into Eq. (64) and

separating the results into their real and imaginary parts yields

$$\dot{a} + \mu a = 0 \tag{66}$$

$$\dot{\beta} = \frac{9\omega_0^2\eta_3 - 10\eta_2^2}{24\omega_0^3}a^2 \tag{67}$$

In the last two equations, the prime symbol denotes the derivative with respect to T_2. Solving Eq. (66) yields

$$a = a_0 e^{-\mu T_2} = a_0 e^{-\hat{\mu}t} \tag{68}$$

Substituting Eq. (68) into Eq. (67) and solving the result equation leads to

$$\beta = \left[\frac{10\widehat{\eta}_2^2 - 9\omega_0^2\widehat{\eta}_3}{48\widehat{\mu}\omega_0^3}\right]a_0^2 e^{-2\hat{\mu}t} + \beta_0 \tag{69}$$

a_0 and β_0 are two constants of integration, which are determined according to the following initial conditions of motion

$$a(0) = \Lambda \tag{70a}$$

$$\beta(0) = 0 \tag{70b}$$

Λ is the maximum amplitude of the nonlinear oscillation. Substituting Eq. (70a) into Eq. (68) leads to

$$\Lambda = a_0 \tag{71}$$

Using Eqs. (69), (70b) and (71) leads to

$$\beta_0 = -\left[\frac{10\widehat{\eta}_2^2 - 9\omega_0^2\widehat{\eta}_3}{48\widehat{\mu}\omega_0^3}\right]\Lambda^2 \tag{72}$$

Substituting Eqs. (71) and (72) into Eq. (69) leads to the following expression for β

$$\beta = \left[\frac{10\widehat{\eta}_2^2 - 9\omega_0^2\widehat{\eta}_3}{48\widehat{\mu}\omega_0^3}\right]\Lambda^2\left(e^{-2\hat{\mu}t} - 1\right) \tag{73}$$

and considering Eq. (64), the solution of Eq. (63) can be written as below

$$q_1 = -\frac{1}{8\omega_0^2}\left[\frac{2\eta_2^2}{3\omega_0^2} + \eta_3\right]A^3 e^{3i\omega_0 T_0} + cc \tag{74}$$

Finally, by substituting Eqs. (58), (62) and (74) into Eq. (54) together with Eq. (65), leads to the following approximate solution

$$q = \Lambda e^{-\hat{\mu}t}\, cos\, \Omega(t) + \frac{\widehat{\eta}_2}{6\omega_0^2}\Lambda^2 e^{-2\hat{\mu}t}\, cos\, 2\,\Omega(t) - \frac{1}{2}\Lambda^3 e^{-3\hat{\mu}t}\left[\frac{\widehat{\eta}_2^2}{3\omega_0^2} + \widehat{\eta}_3\right] cos\, 3\,\Omega(t) \tag{75}$$

where

$$\Omega(t) = \omega_0 t + \beta$$

3. Numerical results

In this section, we perform some numerical computations for a microscale fiber reinforced composite laminated beam with a stacking sequence [90/90/90], under a uniform temperature rise $\Delta T = 29\,C$. The microscale beam is made by three layers of width $b = 25\mu m$, length $L = 900\mu m$, material length scale parameter $l = 17.6\mu m$, and total thickness $h = 30\mu m$. As mentioned before, each layer of the microbeam, has the same thickness. The laminated composite microbeam is also made of Graphite/Epoxy with thermo-mechanical properties, as presented in Eq. (17), with density $\rho = 1536\ \frac{kg}{m^3}$, maximum amplitude of the nonlinear oscillation $\Lambda = 0.10nm$, and the damping coefficient $C_d = 0.005Pa.s$, respectively.

In order to validate the results of the current work, a comparison study is carried out. By neglecting the thermal load in Eq. (47), the fundamental frequencies for the simply supported composite laminated microbeam are obtained for different values of slenderness ratio and compared with the results presented by Chen and Li [49], as shown in Table 1. Looking from an overall perspective, it is evident that there is a good agreement has been achieved between the present results and

Table 1
Comparison study: Fundamental frequencies of composite laminated micro beam. ($l = 2.0\mu m$) [90/0/90].

$\frac{L}{h}$	Fundamental frequencies ($M\,Hz$)	
	Present work	Chen and Li [49]
15.0	1.2861	1.2870
25.0	0.4630	0.4633
35.0	0.2362	0.2364
50.0	0.1157	0.1158
75.0	0.0514	0.0515
100.0	0.0289	0.0290

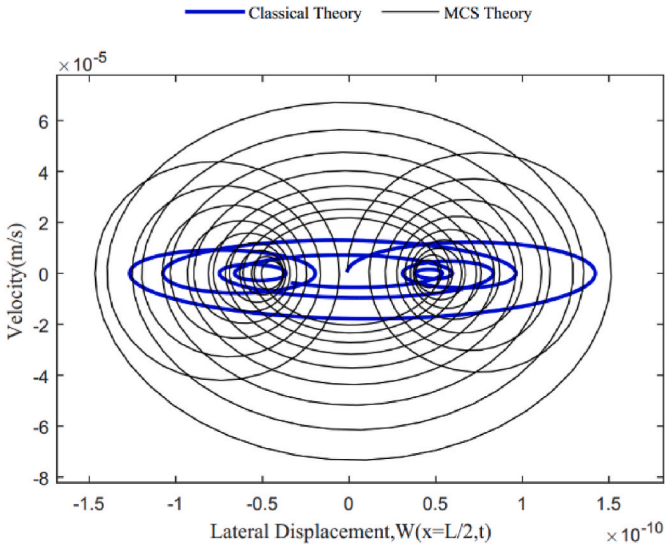

Fig. 3. Effect of length scale parameter on the phase trajectory of the microscale composite laminated beam.

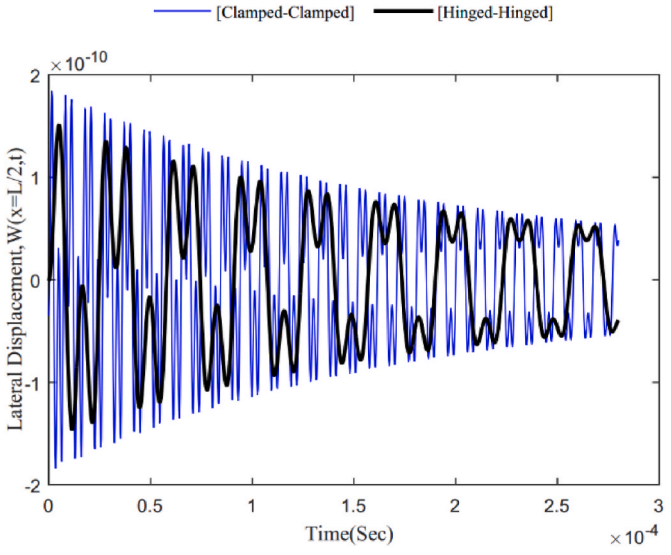

Fig. 4. Effect of boundary conditions on the time history of the microscale composite laminated beam.

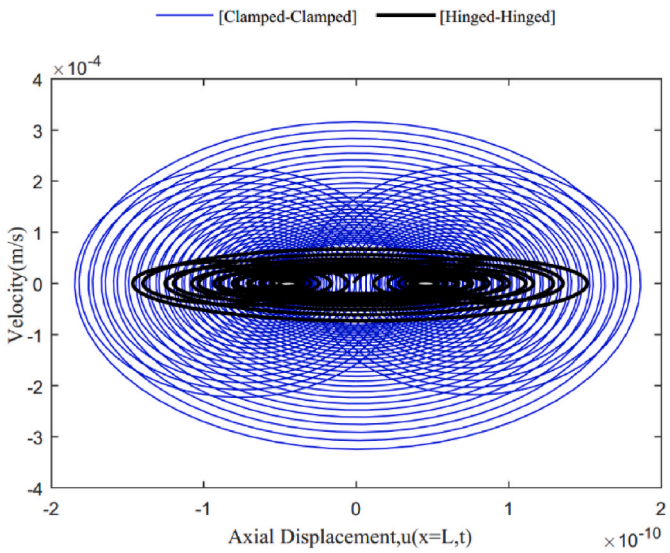

Fig. 5. Effect of boundary conditions on the phase trajectory of the microscale composite laminated beam.

predictions by Chen and Li [49], validating the present model.

Figs. 2 and 3 exhibit the effect of the material length scale parameter on the time history and phase plane trajectory of the system, respectively. As visible from these figures, a period-doubling bifurcation of four-cycle oscillations takes place while the oscillation amplitude decreases in presence of a damping effect. Moreover, results show that the modified couple stress theory predicts a higher nonlinear frequency, higher lateral dynamic deflection and higher velocity of the nonlinear oscillation compared with a classical theory.

Figs. 4 and 5 aim at investigating the effect of the boundary conditions on the time history and phase plane trajectory of the system, respectively.

The results show that, both the lateral dynamic deflection and nonlinear frequency increase by changing the boundary conditions from Hinged-Hinged to Clamped-Clamped. At the same time, results demonstrated that moving from simply-supports to clamped-supports, the phase trajectory expands outward and the velocity of the nonlinear oscillation considerably increases. However, the system remains at the damped period doubling bifurcation for four cycle oscillations states.

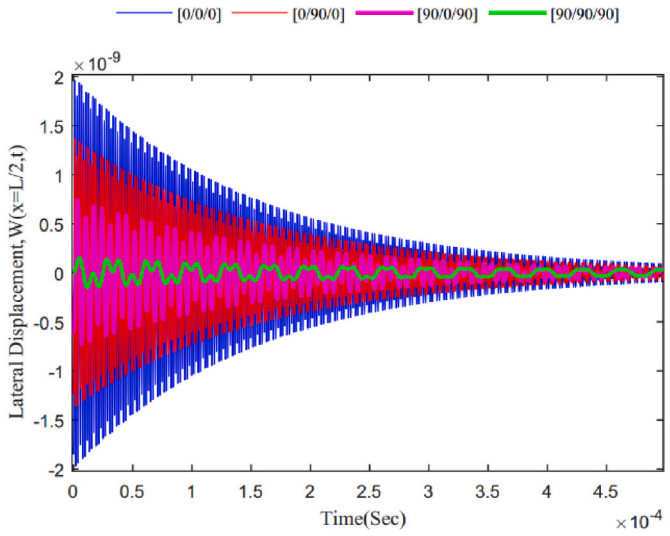

Fig. 6. Effect of stacking sequence (cross-ply) on the time history of the microscale composite laminated beam.

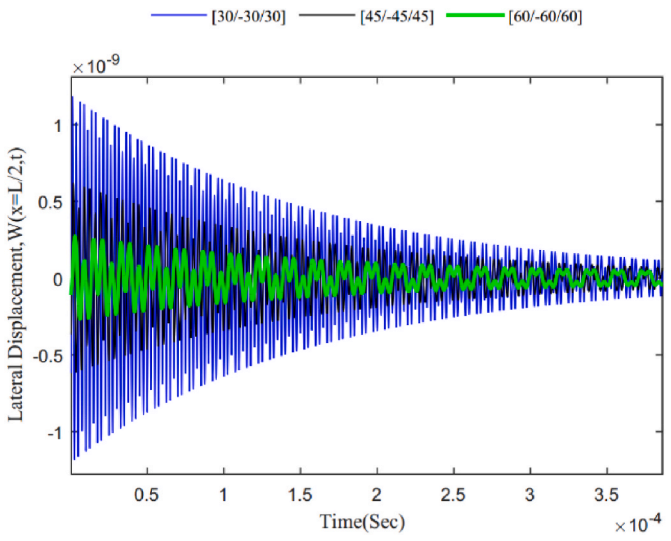

Fig. 7. Effect of stacking sequence (angle-ply) on the time history of the microscale composite laminated beam.

In order to investigate the impact of the stacking sequence on the nonlinear dynamic behavior of the system, Figs. 6 and 7 represent the time histories for different cross ply and angle ply lay-ups, respectively.

As can be seen, the stacking sequence affects significantly the nonlinear dynamic behavior of the system. The results show that the microscale composite laminated beam with [0/0/0] lays-ups has the highest dynamic deflection and the highest nonlinear frequency, followed by [0/90/0], [+30/-30/+30], [90/0/90], [+45/-45/+45], and [+60/-60/+60]. However, the microscale composite laminated beam with [90/90/90] lays-ups has the lowest dynamic deflection and the lowest nonlinear frequency. Moreover, it can be noticed that the system still remains at the period doubling bifurcation for four cycle oscillations state, despite the variation of the stacking sequence.

Figs. 8 and 9 show the effect of a uniform temperature increase on the time history and phase plane trajectory of the system, respectively. The results show that the lateral dynamical deflection and the nonlinear frequency decrease for an increased temperature. As also visible from results, for an increased temperature, the phase plane trajectory shrinks inward and the velocity of the nonlinear oscillation decreases

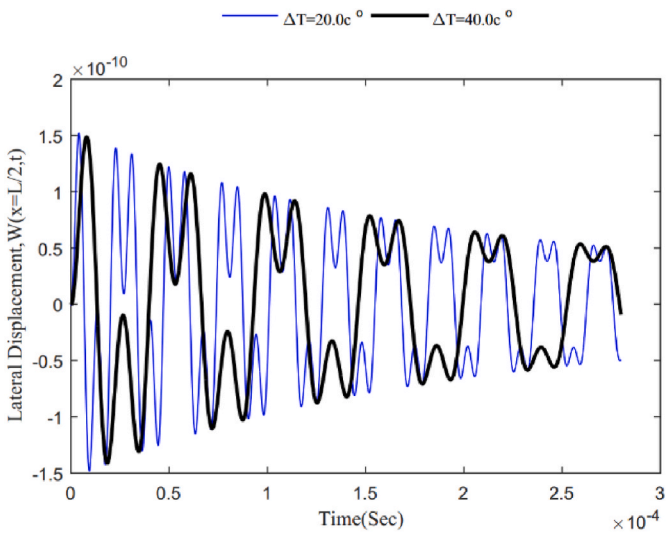

Fig. 8. Effect of uniform temperature rise on the time history of the microscale composite laminated beam.

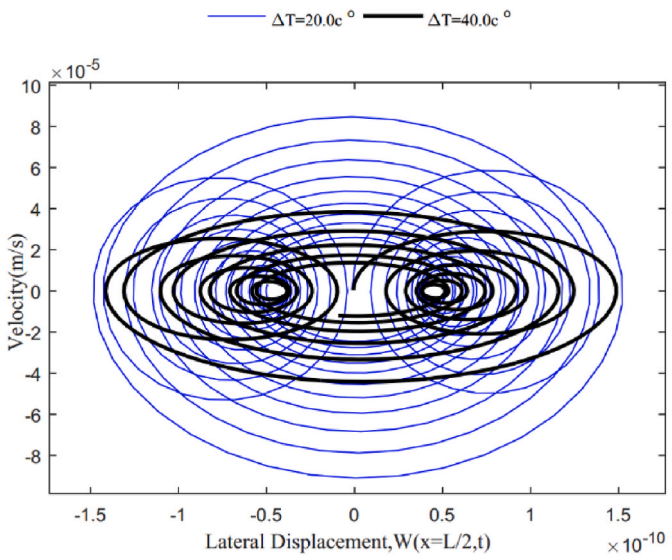

Fig. 9. Effect of uniform temperature rise on the phase plane trajectory of the microscale composite laminated beam.

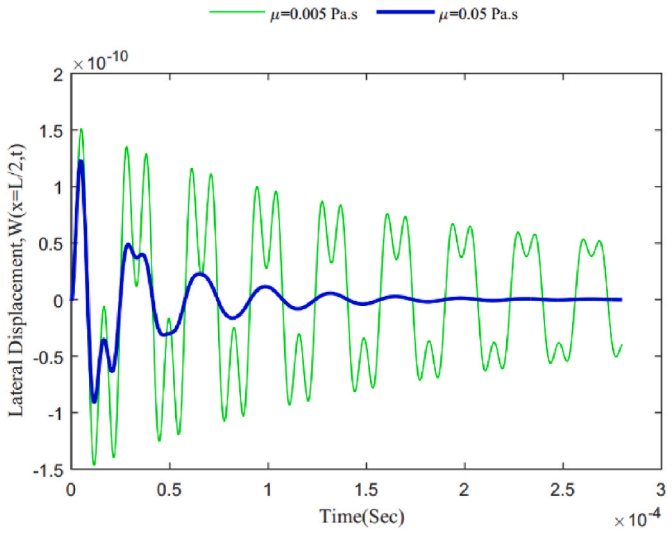

Fig. 10. Effect of damping coefficient on the time history of the microscale composite laminated beam.

significantly.

Finally, Figs. 10 and 11 exhibit the effect of the damping term on the time history and the phase plane trajectory of the system, respectively. As also expected, the results show that the lateral dynamical deflection decreases, for an increased damping coefficient, and at the same time, the dynamics of the system changes from a period-doubling bifurcation for four cycle oscillation to a stable focus.

Indeed, when the system is placed in a high viscous medium, it initially shows a damped period doubling bifurcation for a four-cycle oscillation behavior. However, the dynamic response of the system changes, during the time, up to a final stable condition.

4. Conclusion

The present work has focused on the nonlinear dynamic response of fiber-reinforced composite laminated microbeams in thermal condition, while considering the dependence of the material properties on temperature. The governing nonlinear partial differential equations of the problem have been determined, based on the Euler-Bernoulli beam

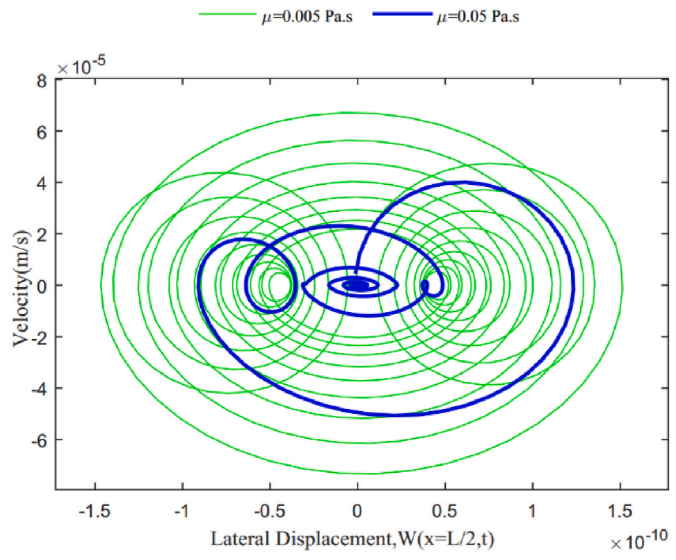

Fig. 11. Effect of damping coefficient on the phase plane trajectory of the microscale composite laminated beam.

theory, modified couple stress theory and von Kármán-type geometrical nonlinearities. The governing equations of the problem have been reduced to a single equation by neglecting the axial inertia. This equation has been discretized according to the Galerkin method, and it has been solved analytically using the multiple time scales (MTS) method. A parametric investigation has focused on the sensitivity of the dynamic response and phase plane trajectory to the material length scale parameter, uniform temperature rise, width of the microscale beam, but also to the stacking sequence. Based on the numerical study, the most significant conclusions can be summarized as follows. First of all, a period-doubling bifurcation is observed for four-cycle oscillations, where the amplitude of the oscillation decreases due to the damping effect. The modified couple stress theory predicts a higher nonlinear frequency, a higher lateral dynamic deflection and a higher velocity of the nonlinear oscillation, compared to the classical theory. In addition, moving from simply supports to clamped supports, the lateral dynamic deflection, nonlinear frequency and velocity of the nonlinear oscillation increases considerably. It is also observed that the microscale composite laminated beam with [0/0/0] lays-ups features the highest dynamic deflection and highest nonlinear frequency, followed by [0/90/0], [+30/-30/+30], [90/0/90], [+45/-45/+45], and [+60/-60/+60] lamination schemes. However, the microscale composite laminated beam with [90/90/90] lays-ups shows the lowest dynamic deflection and the lowest nonlinear frequency. For an increased temperature, the lateral dynamical deflection decreases together with the nonlinear frequency and nonlinear oscillation velocity. As also expected, for an increased damping coefficient, the lateral dynamic deflection decreases, and the dynamic of the system changes from period-doubling bifurcation for four-cycle oscillations to a stable condition.

Conflict of interest and authorship confirmation form

All authors have participated in (a) conception and design, or analysis and interpretation of the data; (b) drafting the article or revising it critically for important intellectual content; and (c) approval of the final version.

This manuscript has not been submitted to, nor is under review at, another journal or other publishing venue.

The authors have no affiliation with any organization with a direct or indirect financial interest in the subject matter discussed in the manuscript.

CRediT authorship contribution statement

Mehdi Alimoradzadeh: Writing – original draft, Validation, Investigation, Formal analysis, Data curation. **Francesco Tornabene:** Writing – review & editing, Validation, Supervision, Methodology, Investigation, Formal analysis, Conceptualization. **Rossana Dimitri:** Writing – review & editing, Validation, Supervision, Methodology, Investigation, Formal analysis, Conceptualization.

Declaration of competing interest

The authors declare that they have no known competing financial interests or personal relationships that could have appeared to influence the work reported in this paper.

Data availability

No data was used for the research described in the article.

References

[1] F. Tornabene, M. Viscoti, R. Dimitri, On the importance of the recovery procedure in the semi-analytical solution for the static analysis of curved laminated panels: comparison with 3D finite elements, Materials 17 (2024) 588.
[2] F. Tornabene, M. Viscoti, R. Dimitri, General boundary conditions implementation for the static analysis of anisotropic doubly-curved shells resting on a Winkler foundation, Compos. Struct. 322 (2023) 117198.
[3] F. Tornabene, M. Viscoti, R. Dimitri, Static analysis of anisotropic doubly-curved shell subjected to concentrated loads employing higher order layer-wise theories, CMES-comp. Model, Eng. Sci. 134 (2) (2023) 1393–1468.
[4] F. Tornabene, M. Viscoti, R. Dimitri, Static analysis of anisotropic doubly-curved shells with arbitrary geometry and variable thickness resting on a Winkler-Pasternak support and subjected to general loads, Eng. Anal. Bound. Elem. 140 (2022) 618–673.
[5] M. Alimoradzadeh, S.D. Akbas, Nonlinear dynamic behavior of functionally graded beams resting on nonlinear viscoelastic foundation under moving mass in thermal environment, Struct. Eng. Mech. 81 (2022) 705.
[6] M. Alimoradzadeh, Ş.D. Akbaş, Superharmonic and subharmonic resonances of atomic force microscope subjected to crack failure mode based on the modified couple stress theory, Eur. Phys. J. Plus 136 (2021) 536.
[7] M. Alimoradzadeh, S.D. Akbas, S.M. Esfrajani, Nonlinear dynamic and stability of a beam resting on the nonlinear elastic foundation under thermal effect based on the finite strain theory, Struct. Eng. Mech. 80 (2021) 275–284.
[8] A. Mahmure, A.H. Sofiyev, N. Fantuzzi, N. Kuruoglu, Primary resonance of double-curved nanocomposite shells using nonlinear theory and multi-scales method: modeling and analytical solution, Int. J. Non Lin. Mech. 137 (2021) 103816.
[9] A.H. Sofiyev, M. Avey, N. Kuruoglu, An approach to the solution of nonlinear forced vibration problem of structural systems reinforced with advanced materials in the presence of viscous damping, Mech. Syst. Signal Process. 161 (2021) 107991.
[10] B. Gia Phi, D. Van Hieu, H.M. Sedighi, A.H. Sofiyev, Size-dependent nonlinear vibration of functionally graded composite micro-beams reinforced by carbon nanotubes with piezoelectric layers in thermal environments, Acta Mech. 233 (6) (2022) 2249–2270.
[11] A.H. Sofiyev, Nonlinear forced response of doubly-curved laminated panels composed of CNT patterned layers within first order shear deformation theory, Thin-Walled Struct. 193 (2023) 11227.
[12] N.D. Duc, P.H. Cong, Nonlinear vibration of thick FGM plates on elastic foundation subjected to thermal and mechanical loads using the first-order shear deformation plate theory, Cogent Eng. 2 (2015) 1045222.
[13] M. Alimoradzade, S.D. Akbas, Nonlinear thermal vibration of FGM beams resting on nonlinear viscoelastic foundation, Steel Compos. Struct. 44 (2022) 543–553.
[14] Y. Chai, F. Li, Z. Song, Nonlinear vibrations, bifurcations and chaos of lattice sandwich composite panels on Winkler–Pasternak elastic foundations with thermal effects in supersonic airflow, Meccanica 54 (2019) 919–944.
[15] B. Ameri, M. Moradi, R. Talebitooti, Effect of honeycomb core on free vibration analysis of fiber metal laminate (FML) beams compared to conventional composites, Compos. Struct. 261 (2021) 113281.
[16] M. Amabili, G. Ferrari, M.H. Ghayesh, C. Hameury, H.H. Zamal, Nonlinear vibrations and viscoelasticity of a self-healing composite cantilever beam: theory and experiments, Compos. Struct. 294 (2022) 115741.
[17] M. Alimoradzadeh, S.D. Akbas, Superharmonic and subharmonic resonances of a carbon nanotube-reinforced composite beam, Adv. Nano Res. 12 (2022) 353–363.
[18] M. Alimoradzadeh, F. Tornabene, S.M. Esfarjani, R. Dimitri, Finite strain-based theory for the superharmonic and subharmonic resonance of beams resting on a nonlinear viscoelastic foundation in thermal conditions, and subjected to a moving mass loading, Int. J. Non Lin. Mech. 148 (2023) 104271.
[19] M. Alimoradzadeh, Ş.D. Akbaş, Thermal nonlinear dynamic and stability of carbon nanotube reinforced composite beams, Steel Compos. Struct. 46 (2023) 637–647.
[20] M. Alimoradzadeh, H. Heidari, F. Tornabene, R. Dimitri, Thermo-mechanical buckling and non-linear free oscillation of functionally graded fiber-reinforced composite laminated (FG-FRCL) beams, Appl. Sci. 13 (2023) 4904.
[21] M. Alimoradzadeh, Ş.D. Akbaş, Nonlinear free vibration analysis of a composite beam reinforced by carbon nanotubes, Steel Compos. Struct. 46 (2023) 335–344.
[22] M. Alimoradzadeh, S.D. Akbas, Nonlinear vibration analysis of carbon nanotube-reinforced composite beams resting on nonlinear viscoelastic foundation, Geomech. Eng. 32 (2023) 125–135.
[23] S. Lee, J.H. Kim, Thermomechanical vibration and stability of effectively homogenized FGM beam with temperature dependent shear correction factors, J. Compos. Mater. 57 (2023) 253–264.
[24] S. Kong, S. Zhou, Z. Nie, K. Wang, The size-dependent natural frequency of Bernoulli–Euler micro-beams, Int. J. Eng. Sci. 46 (2008) 427–437.
[25] M. Alimoradzadeh, M. Salehi, S. Mohammadi Esfarjani, Vibration analysis of FG micro-beam based on the third order shear deformation and modified couple stress theories, J. Sim. Anal. Novel Technol. Mech. Eng. 10 (2017) 51–66.
[26] M. Alimoradzadeh, M. Salehi, S.M. Esfarjani, Nonlinear vibration analysis of axially functionally graded microbeams based on nonlinear elastic foundation using modified couple stress theory, Period. Polytech. - Mech. Eng. 64 (2020) 97–108.
[27] M. Alimoradzadeh, S.D. Akbas, Nonlinear dynamic responses of cracked atomic force microscopes, Struct. Eng. Mech. 82 (2022) 747–756.
[28] M. Alimoradzadeh, H. Heidari, F. Tornabene, R. Dimitri, Nonlinear dynamic study of non-uniform microscale CNTR composite beams based on a modified couple stress theory, Int. J. Non Lin. Mech. (2023) 104477.
[29] Ö. Civalek, B. Uzun, M.Ö. Yaylı, B. Akgöz, Size-dependent transverse and longitudinal vibrations of embedded carbon and silica carbide nanotubes by nonlocal finite element method, Europ. Phys. J. Plus 135 (2020) 381.
[30] P. Kudela, M. Radzienski, W. Ostachowicz, Wave propagation modeling in composites reinforced by randomly oriented fibers, J. Sound Vib. 414 (2018) 110–125.
[31] L. Brinson, W. Lin, Comparison of micromechanics methods for effective properties of multiphase viscoelastic composites, Compos. Struct. 41 (3–4) (1998) 353–367.
[32] R. Christensen, Viscoelastic properties of heterogeneous media, J. Mech. Phys. Solid. 17 (1) (1969) 23–41.
[33] M. Samadpour, H. Asadi, Q. Wang, Nonlinear aero-thermal flutter postponement of supersonic laminated composite beams with shape memory alloys, Eur. J. Mech. Solid. 57 (2016) 18–28.
[34] H. Asadi, A.R. Beheshti, On the nonlinear dynamic responses of FG-CNTRC beams exposed to aerothermal loads using third-order piston theory, Acta Mech. 229 (2018) 2413–2430.
[35] G. Yao, Y.M. Zhang, C.Y. Li, Z. Yang, Stability analysis and vibration characteristics of an axially moving plate in aero-thermal environment, Acta Mech. 227 (2016) 3517–3527.
[36] G. Yao, Z. Xie, L. Zhu, Y. Zhang, Nonlinear vibrations of an axially moving plate in aero-thermal environment, Nonlinear Dynam. 105 (2021) 2921–2933.
[37] M. Alimoradzadeh, F. Tornabene, R. Dimitri, Nonlinear axial-lateral coupled vibration of functionally graded-fiber reinforced composite laminated (FG-FRCL) beams subjected to aero-thermal loads, Int. J. Non Lin. Mech. 159 (2024) 104612.
[38] R. Fernandes, S.M. Mousavi, S. El-Borgi, Free and forced vibration nonlinear analysis of a microbeam using finite strain and velocity gradients theory, Acta Mech. 227 (2016) 2657–2670.
[39] S. Ramezani, A micro scale geometrically non-linear Timoshenko beam model based on strain gradient elasticity theory, Int. J. Non Lin. Mech. 47 (2012) 863–873.
[40] Y.H. Dong, Y.F. Zhang, Y.H. Li, An analytical formulation for postbuckling and buckling vibration of micro-scale laminated composite beams considering hygrothermal effect, Compos. Struct. 170 (2017) 11–25.
[41] M.W. Hyer, S.R. White, Stress Analysis of Fiber-Reinforced Composite Materials, DEStech Publications, Inc, 2009.
[42] H.S. Shen, Thermal postbuckling behavior of imperfect shear deformable laminated plates with temperature-dependent properties, Comput. Methods Appl. Mech. Eng. 190 (2001) 5377–5390.
[43] S.F. Nikrad, H. Asadi, Thermal postbuckling analysis of temperature dependent delaminated composite plates, Thin-Walled Struct. 97 (2015) 296–307.
[44] W.J. Chen, X.P. Li, Size-dependent free vibration analysis of composite laminated Timoshenko beam based on new modified couple stress theory, Arch. Appl. Mech. 83 (2013) 431–444.
[45] M. Samadpour, H. Asadi, Q. Wang, Nonlinear aero-thermal flutter postponement of supersonic laminated composite beams with shape memory alloys, Eur. J. Mech. Solid. 57 (2016) 18–28.
[46] H. Norouzi, D. Younesian, Chaotic vibrations of beams on nonlinear elastic foundations subjected to reciprocating loads, Mech. Res. Commun. 69 (2015) 121–128.
[47] M. Şimşek, Nonlinear static and free vibration analysis of microbeams based on the nonlinear elastic foundation using modified couple stress theory and He's variational method, Compos. Struct. 112 (2014).
[48] A.H. Nayfeh, D.T. Mook, P. Holmes, Nonlinear oscillations, Wiley Publishing, https://doi.org/10.1002/9783527617586..
[49] W.J. Chen, X.P. Li, Size-dependent free vibration analysis of composite laminated Timoshenko beam based on new modified couple stress theory, Arch. Appl. Mech. 83 (2013) 431–444.